

0^{++} Resonances Observed at BES

B. S. Zou (for BES Collaboration)

Institute of High Energy Physics, CAS, Beijing 100049, China

Abstract. In last 10 years, 0^{++} resonances have been observed and studied at BES in many processes, such as $J/\psi \rightarrow \gamma\pi^+\pi^-\pi^+\pi^-$, $\gamma\pi^+\pi^-$, $\gamma\pi^0\pi^0$, γK^+K^- , $\gamma K_S^0 K_S^0$, $\gamma\omega\phi$, $\omega\pi^+\pi^-$, ωK^+K^- , $\phi\pi^+\pi^-$, ϕK^+K^- , $\psi(2S) \rightarrow J/\psi\pi^+\pi^-$, $\chi_{c0} \rightarrow \pi^+\pi^-K^+K^-$, $\pi^+\pi^-\pi^+\pi^-$ etc.. The results on 0^{++} resonances observed at BES are reviewed.

Keywords: Scalar meson, glueball, J/ψ decays

PACS: 14.40.Cs, 13.25.Gv, 13.20.Gd

INTRODUCTION

The study of the isoscalar 0^{++} resonances is of crucial importance for understanding the whole hadron spectrum. The lightest $q\bar{q}$ spatial excited state, the lightest glueball, and the lightest tetra-quark state, all are expected to have such quantum numbers of vacuum. Up to now, there are five isoscalar 0^{++} resonances ($\sigma/f_0(600)$, $f_0(980)$, $f_0(1370)$, $f_0(1500)$ and $f_0(1710)$) listed as well-established ones by PDG [1], and four unestablished ones ($f_0(1790)$, $f_0(2020)$, $f_0(2100)$ and $f_0(2200)$). None of them gets a clear picture about its internal structure. They are ascribed as $q\bar{q}$ states, $q^2\bar{q}^2$ states, meson-meson molecules, glueballs, coupled-channel dynamical states, etc.

Among various reactions, three kinds of processes from charmonium decays may play important role for understanding the nature of these scalars and have been studied by BES Collaboration at Beijing Electron-Positron Collider (BEPC). They are ψ radiative decays, ψ hadronic decays against ϕ or ω , and χ_{c0} decays. In the following three sections, we will outline the major physics roles and review main results on scalar resonances from each of them. A brief summary of the information on scalars we deduced from these processes is given in the final section.

0^{++} RESONANCES OBSERVED IN ψ RADIATIVE DECAYS

There are three main physics objectives for ψ radiative decays:

(1) Looking for glueballs and hybrids. As shown in Fig. 1, after emitting a photon, the $c\bar{c}$ pair is in a $C = +1$ state and decays to hadrons dominantly through two gluon intermediate states. Simply counting the power of α_s , we know that glueballs should have the largest production rate, hybrids the second, then the ordinary $q\bar{q}$ mesons.

(2) Completing $q\bar{q}$ meson spectroscopy and studying their production and decay rates, which is crucial for understanding their internal structure and confinement.

(3) Extracting $gg \leftrightarrow q\bar{q}$ coupling from perturbative energy region of above 3.6 GeV to nonperturbative region of 0.3 GeV. This may show us some phenomenological pattern

for the smooth transition from perturbative QCD to strong nonperturbative QCD.

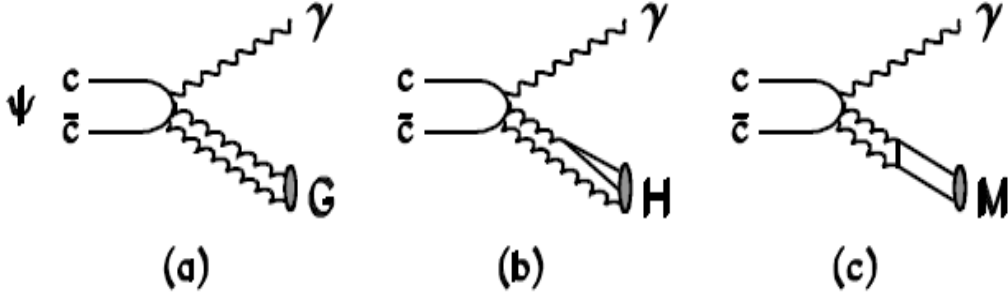


FIGURE 1. ψ radiative decays to (a) glueball, (b) hybrid, and (c) $q\bar{q}$ meson.

For the study of the isoscalar 0^{++} resonances from the J/ψ radiative decays, we have studied the largest radiative decay channel $J/\psi \rightarrow \gamma 4\pi$, the simplest ones $J/\psi \rightarrow \gamma\pi\pi$, $\gamma K\bar{K}$, and the exotic doubly OZI suppressed one $J/\psi \rightarrow \gamma\omega\phi$. Partial wave analysis has been performed for the $\gamma\pi^+\pi^-\pi^+\pi^-$ channel of BES I data [2], $\gamma\pi^+\pi^-$ [3], γK^+K^- [4] and $\gamma\omega\phi$ [5] channels of BES II data.

The invariant mass spectra and 0^{++} partial wave contribution for $J/\psi \rightarrow \gamma\pi^+\pi^-\pi^+\pi^-$ at BES I [2] and $\gamma\pi^+\pi^-$ at BES II [3] are shown in Fig.2. The two channels have a similar pattern of three-peak structure for the 0^{++} partial wave contribution. The fitted mass and width for these 0^{++} peaks in $\gamma\pi^+\pi^-\pi^+\pi^-$ [2] and $\gamma\pi^+\pi^-$ [3] channels are listed in Table 1. The results from the two channels are consistent with each other within their error bars and with those from a reanalysis of MARK III data for the $\gamma\pi^+\pi^-\pi^+\pi^-$ channel [6]. The 2π invariant mass spectrum for the $\gamma\pi^0\pi^0$ channel is similar to that from the $\gamma\pi^+\pi^-$ channel as shown in Fig. 3.

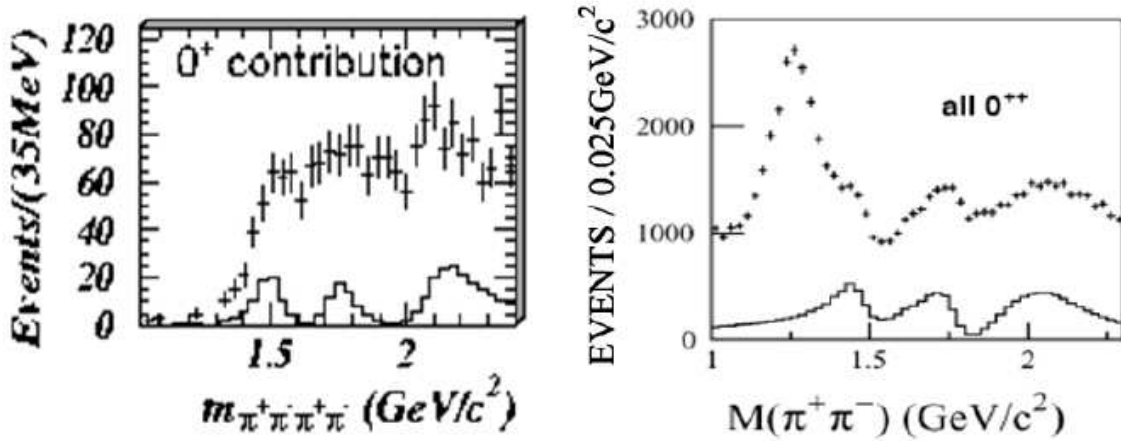


FIGURE 2. Invariant mass spectra and 0^{++} partial wave contribution for $J/\psi \rightarrow \gamma\pi^+\pi^-\pi^+\pi^-$ at BES I [2] (left) and $\gamma\pi^+\pi^-$ at BES II [3] (right)

The invariant mass spectra for the $J/\psi \rightarrow \gamma K^+K^-$ and $\gamma K_S K_S$ channels are shown in Fig. 3. The partial wave analysis has been performed for the mass below 2 GeV [4]. While the peak around 1525 MeV is mainly due to $f_2'(1525)$, the peak around 1740

TABLE 1. Fitted mass and width (in unit of MeV) for the three 0^{++} peaks in $\gamma\pi^+\pi^-\pi^+\pi^-$ [2] and $\gamma\pi^+\pi^-$ [3] channels

resonance	mass [2]	width [2]	mass [3]	width [3]
$f_0(1500)$	1505^{+15}_{-20}	140^{+40}_{-30}	$1466 \pm 6 \pm 16$	$108^{+14}_{-11} \pm 21$
$f_0(1710 \sim 1790)$	1740^{+30}_{-25}	120^{+50}_{-40}	$1765^{+4}_{-3} \pm 11$	$145 \pm 8 \pm 23$
$f_0(2020 \sim 2200)$	2090 ± 30	330 ± 100	2020 PDG	PDG

MeV is dominated by 0^{++} contribution with fitted mass and width as $1740 \pm 4^{+10}_{-25}$ and 166^{+5+15}_{-8-10} MeV, respectively. Recently, the $\gamma\pi^+\pi^-$ and γK^+K^- channels from ψ' decays have also been studied with similar peaks observed [7].

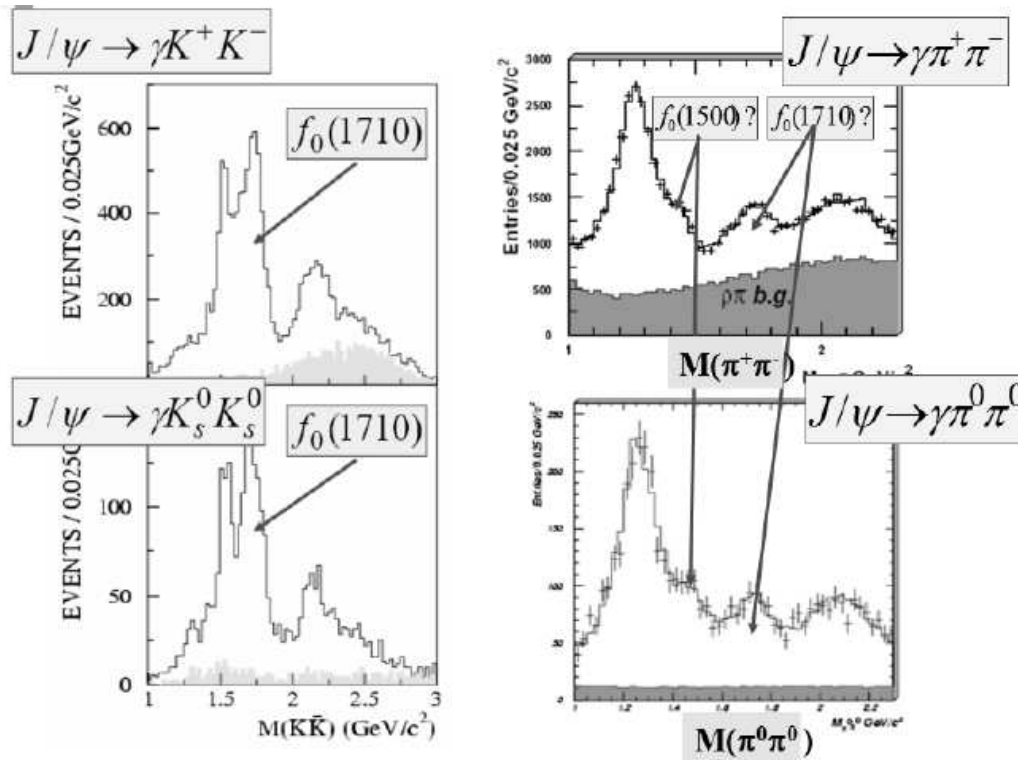


FIGURE 3. Invariant mass spectra for the $J/\psi \rightarrow \gamma K\bar{K}$ [4] and $\gamma\pi\pi$ [3] channels

For the doubly OZI suppressed channel $\gamma\omega\phi$, the Dalitz plot and the $\omega\phi$ invariant mass spectrum are shown in Fig. 4. A clear enhancement near $\omega\phi$ threshold is observed. A partial wave analysis shows that this enhancement favors $J^P = 0^+$ [5]. If fitted with a simple Breit-wigner formulae of constant width, the mass and width are obtained as $M = 1812^{+19}_{-26} \pm 18$ MeV and $\Gamma = 105 \pm 20 \pm 28$ MeV, respectively. Considering possible energy dependence factors caused by threshold and off-shell effects, the possible relation with the sub-threshold $f_0(1710 \sim 1790)$ structure cannot be excluded. But the large branching ratio to this doubly OZI suppressed channel needs some special theoretical attention to identify its nature [8].

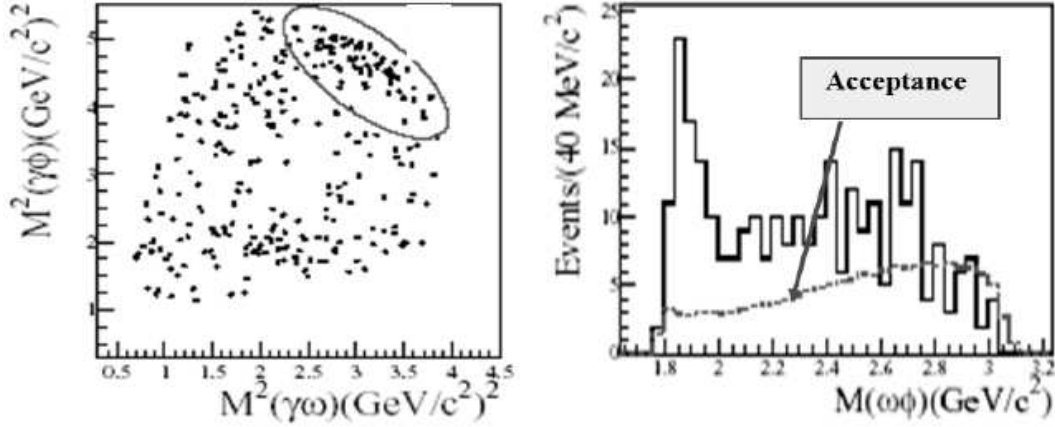


FIGURE 4. Dalitz plot and Invariant mass spectrum for the $J/\psi \rightarrow \gamma\omega\phi$ channel [5].

0^{++} RESONANCES OBSERVED IN ψ HADRONIC DECAYS

For the ψ hadronic decays against ϕ/ω , there are also mainly three physics objectives:

(1) Looking for hybrids. Since ψ decays to hadrons through three gluons, final states involving a hybrid as shown in Fig. 5(a) are expected to have larger production rate than ordinary $q\bar{q}$ mesons as shown in Fig. 5(b,c).

(2) Extracting $u\bar{u} + d\bar{d}$ and $s\bar{s}$ components of associated mesons, M , via $\psi \rightarrow M + \omega/\phi$ as shown in Fig. 5(b,c).

(3) Disfavoring glueball production. We can analyze the quark/gluon content of a particle, M , by comparing its production in $\psi \rightarrow \gamma M$, ωM and ϕM .

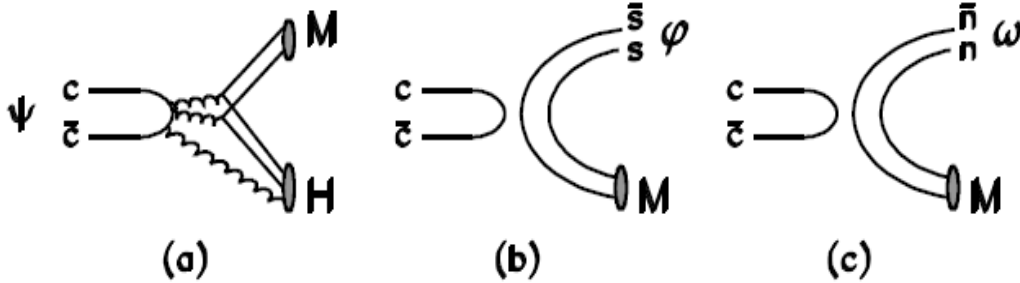


FIGURE 5. ψ hadronic decays to (a) hybrids, (b) $s\bar{s}$, and (c) $n\bar{n} \equiv \frac{1}{\sqrt{2}}(u\bar{u} + d\bar{d})$ mesons.

To investigate the $u\bar{u} + d\bar{d}$ and $s\bar{s}$ components of iso-scalar 0^{++} resonances, we have studied $J/\psi \rightarrow \omega\pi^+\pi^-$ [9], ωK^+K^- [10], $\phi\pi^+\pi^-$ and ϕK^+K^- [11] channels. The invariant mass spectra for these channels are shown in Fig.6. They are similar to the previous ones by MARKIII and DM2 Collaborations, but with much higher statistics.

For $J/\psi \rightarrow \omega\pi^+\pi^-$, there are two clear peaks at 500 MeV and 1275 MeV in the 2π mass spectrum corresponding to the σ and the $f_2(1275)$, respectively. The σ pole

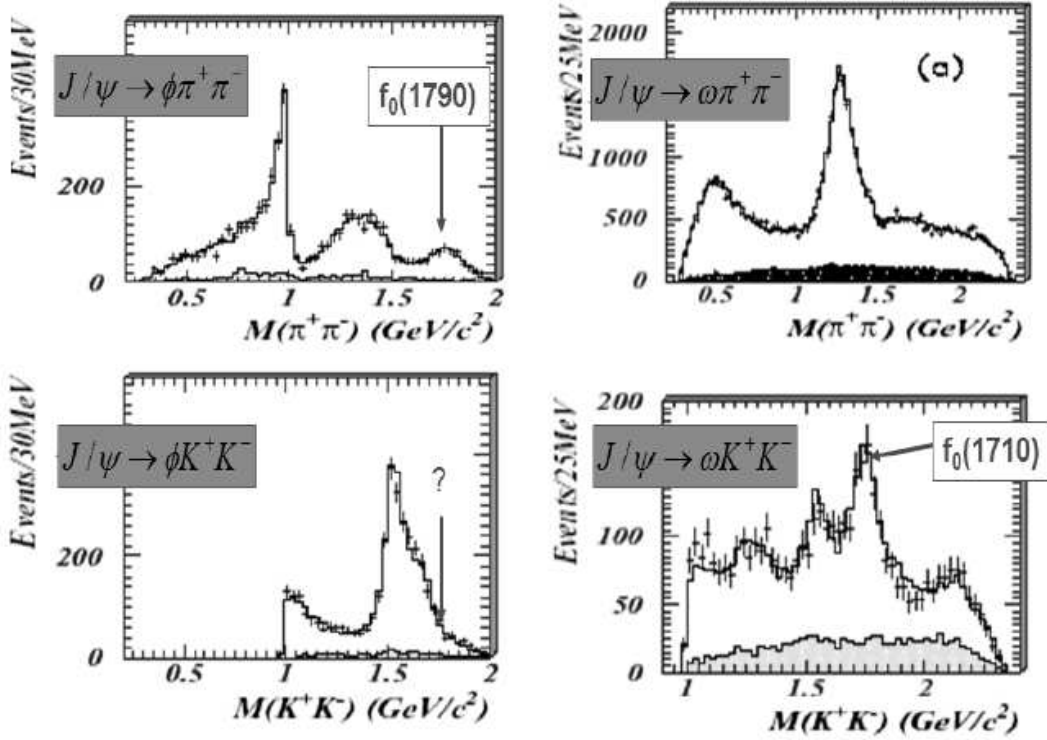


FIGURE 6. Invariant mass spectra for the $J/\psi \rightarrow \phi\pi^+\pi^-$, ϕK^+K^- [11], $\omega\pi^+\pi^-$ [9] and ωK^+K^- [10] channels.

position is determined to be $(541 \pm 39) - i(252 \pm 42)$ MeV from the mean of six analyses [9] by using various parametrizations [12, 13]. It is also consistent with a later study of high statistical data of $\psi' \rightarrow J/\psi\pi^+\pi^-$ [14]. For $J/\psi \rightarrow \omega K^+K^-$, there is a conspicuous signal for $f_0(1710) \rightarrow K^+K^-$. From a combined analysis of these two sets of data, the branching ratio $BR(f_0(1710) \rightarrow \pi\pi)/BR(f_0(1710) \rightarrow K\bar{K})$ is < 0.11 at the 95% confidence level [10].

For the $J/\psi \rightarrow \phi\pi^+\pi^-$ and ϕK^+K^- channels, the $f_0(980)$ is observed clearly in both sets of data, and parameters of the Flatté formula are determined accurately: $M = 0.965 \pm 0.010$ GeV, $g_1 = 0.165 \pm 0.018$ GeV², $g_2/g_1 = 4.21 \pm 0.25 \pm 0.21$. The $\phi\pi\pi$ data also exhibit a strong $\pi\pi$ peak centered at $M = 1335$ MeV. It may be fitted with $f_2(1270)$ and a dominant 0^+ signal made from $f_0(1370)$ interfering with a smaller $f_0(1500)$ component. There is also a state in $\pi\pi$ with $M = 1790^{+40}_{-30}$ MeV and $\Gamma = 270^{+60}_{-30}$ MeV; spin 0 is preferred over spin 2. A particular feature is that $f_0(1790) \rightarrow \pi\pi$ is strong, but there is little or no corresponding signal for decays to $K\bar{K}$. This behavior is incompatible with $f_0(1710)$, which is known to decay dominantly to $K\bar{K}$. So this state, $f_0(1790)$, is distinct from $f_0(1710)$. The $\phi K\bar{K}$ data contain a strong peak due to $f_2'(1525)$. A shoulder on its upper side may be fitted by interference between $f_0(1500)$ and $f_0(1710)$.

The large production rates of $f_2(1275)$ against ω and $f_2'(1525)$ against ϕ demonstrate the flavor filter role of the ψ hadronic decays against ϕ/ω . For the scalar production,

the $\omega\sigma/f_0(600)$ and $\phi f_0(980)$ have the largest branching ratios. This suggests that the $f_0(980)$ has large strangeness content while the $\sigma/f_0(600)$ contains mainly the non-strange quarks, just as expected by various models [15]. It seems indeed that the non-gluoballs are favorably produced in these reactions. While $\phi f_0(1370)$, $\phi f_0(1790)$ and $\omega f_0(1710)$ have also significant production rate, the $f_0(1500)$ is hardly visible in any of these processes.

0^{++} RESONANCES OBSERVED IN χ_{c0} DECAYS

Since the decays of χ_{c0} and χ_{c2} into light hadrons are mainly through intermediate states of two gluons, they are expected to provide the cleanest place for studying gluon-hadronization dynamics. Schematic pictures for the decays of $\chi_{c0,2}$ into meson pairs via the production of different components are shown in Fig.7. The study of these decays may also shed light on the internal structures of the produced mesons.

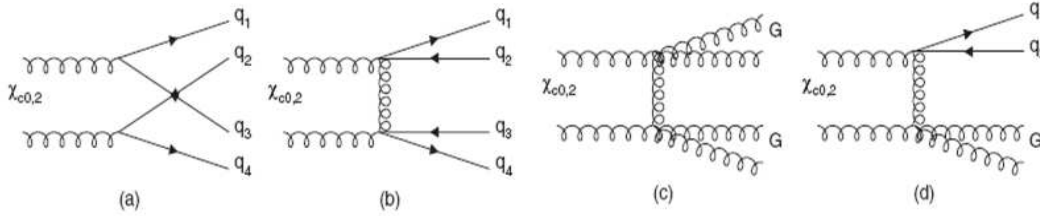


FIGURE 7. Schematic pictures for the decays of $\chi_{c0,2}$ into meson pairs via the production of different components [16].

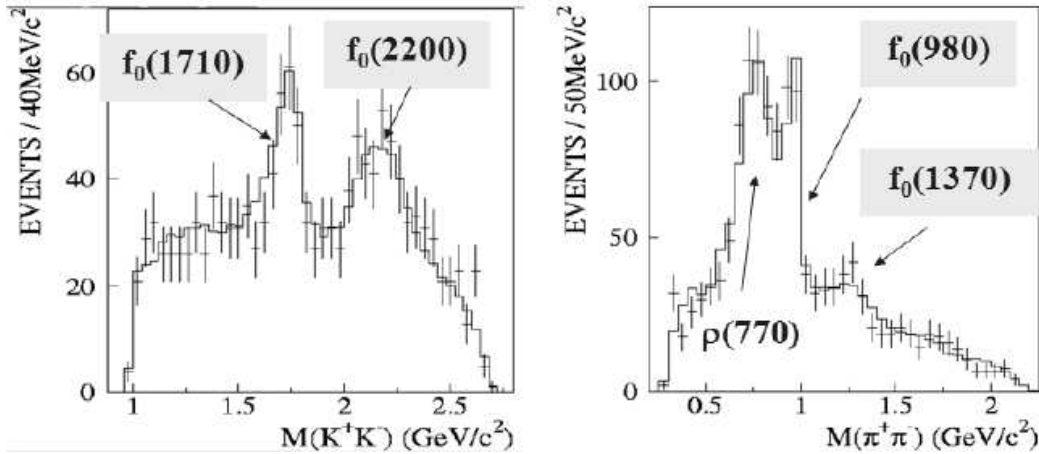


FIGURE 8. Invariant mass spectra of K^+K^- and $\pi^+\pi^-$ for the $\chi_{c0} \rightarrow \pi^+\pi^-K^+K^-$ decays [17].

For the scalar resonance production, we have studied the $\chi_{c0} \rightarrow \pi^+\pi^-K^+K^-$ [17] and $\pi^+\pi^-\pi^+\pi^-$ [18] decays. Partial wave analysis has been performed for the $\chi_{c0} \rightarrow \pi^+\pi^-K^+K^-$ decays. The largest meson pair production rates are found for $K_0^*(1430)\bar{K}_0^*(1430)$, $K_0^*(1430)\bar{K}_2^*(1430) + c.c.$, and $K^*(892)\bar{K}^*(892)$. So it seems again that the non-gluoballs are favorably produced. The invariant mass spectra of K^+K^- and $\pi^+\pi^-$ for the $\chi_{c0} \rightarrow \pi^+\pi^-K^+K^-$ decays are shown in Fig.8. Peaks due to $f_0(1710)$

and $f_0(2200)$ in K^+K^- invariant mass spectrum and ρ , $f_0(980)$ and $f_0(1370)$ in $\pi\pi$ invariant mass spectrum are clearly visible. For the $\chi_{c0} \rightarrow \pi^+\pi^-\pi^+\pi^-$, the peaks due to ρ , $f_0(980)$ and $f_0(1370)/f_2(1270)$ are also visible in the invariant $\pi^+\pi^-$ mass spectrum [18] as shown in Fig.9(a). For the $\chi_{c2} \rightarrow \pi^+\pi^-\pi^+\pi^-$, only the ρ peak is predominant as shown in Fig.9(b) without any obvious information on f_0 resonances.

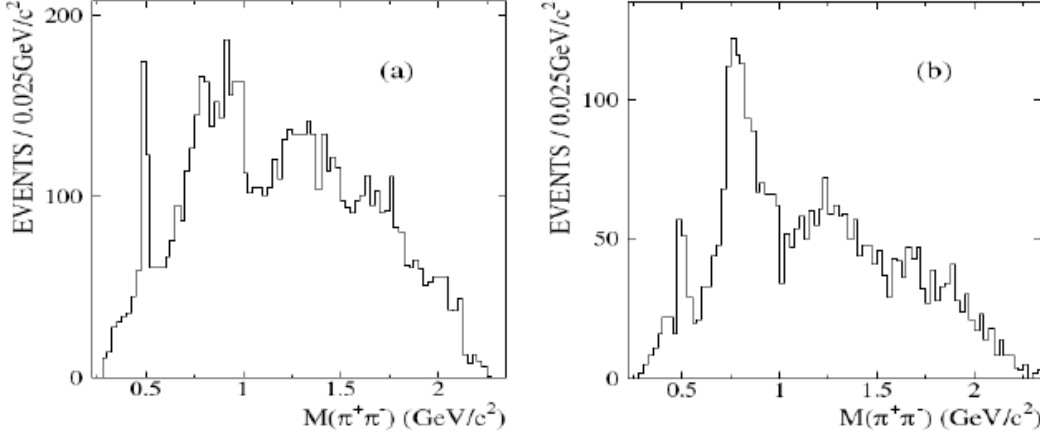


FIGURE 9. Projections of $\pi^+\pi^-$ invariant mass under the (a) χ_{c0} and (b) χ_{c2} peaks (two entries per event) for $\psi' \rightarrow \pi^+\pi^-\pi^+\pi^-$ [18].

SUMMARY

The ψ radiative decays are expected to be the best place to look for glueballs. Three 0^{++} peaks are observed around $f_0(1500)$, $f_0(1710)/f_0(1790)$ and $f_0(2020)/f_0(2100)$ in various ψ radiative decays.

Both ψ hadronic decays against ϕ/ω and χ_{c0} decays seem favoring the non-glueball production. For ψ hadronic decays against ϕ/ω , the $\sigma/f_0(600)$, $f_0(980)$, $f_0(1370)$, $f_0(1710)$ and $f_0(1790)$ resonances are clearly observed. For the $\chi_{c0} \rightarrow \pi^+\pi^-K^+K^-$ and $\pi^+\pi^-\pi^+\pi^-$ decays, the $f_0(980)$, $f_0(1370)$, $f_0(1710)/f_0(1790)$, and $f_0(2200)$ resonances are clearly seen.

The fact that the $f_0(1500)$ is produced strongly only in the glueball favorable ψ radiative decays and weaker than other f_0 resonances in the non-glueball favorable reactions deserves further attention. To study $f_0 \rightarrow \eta\eta$, $\eta\eta'$, $\gamma\phi$, $\gamma\rho$, $\gamma\omega$ from ψ radiative decays at BESIII will shed important light on the nature of these 0^{++} resonances [19].

ACKNOWLEDGMENTS

The BES collaboration thanks the staff of BEPC and computing center for their hard efforts. This work is supported in part by the National Natural Science Foundation of China under contracts Nos. 10491300, 10225524, 10225525, 10425523, 10625524, 10521003, the Chinese Academy of Sciences under contract No. KJ 95T-03, the 100 Talents Program of CAS under Contract Nos. U-11, U-24, U-25, and the Knowledge

Innovation Project of CAS under Contract No. U-602 (IHEP), the National Natural Science Foundation of China under Contract No. 10225522 (Tsinghua University), and the Department of Energy under Contract No. DE-FG02-04ER41291 (U. Hawaii).

REFERENCES

1. Particle Data Group, *J. Phys.* G33 (2006) 1.
2. J. Z. Bai et al. (BES Collaboratin), *Phys. Lett.* B472 (2000) 207.
3. M. Ablikim et al. (BES Collaboration), *Phys. Lett.* B 642 (2006) 441.
4. J. Z. Bai et al. (BES Collaboration), *Phys.Rev.D*68 (2003) 052003.
5. M. Ablikim et al. (BES Collaboration), *Phys. Rev. Lett.* 96 (2006) 162002.
6. D. V. Bugg et al., *Phys. Lett.* B353 (1995) 378.
7. M. Ablikim et al. (BES Collaboration), arXiv: 0710.2324 [hep-ex].
8. B. A. Li, *Phys. Rev. D*74 (2006) 054017; P. Bicudo et al., *Eur. Phys. J. C*52 (2007) 363; K. T. Chao, hep-ph/0602190; D. V. Bugg, hep-ph/0603018; X. G. He et al., *Phys. Rev. D*73 (2006) 114026; Q. Zhao et al., *Phys. Rev. D*74 (2006) 114025; J. Rosner, *Phys. Rev. D*74 (2006) 076006.
9. M. Ablikim et al. (BES Collaboration), *Phys.Lett.* B598 (2004) 149.
10. M. Ablikim et al. (BES Collaboration), *Phys. Lett.* B603 (2004) 138.
11. M. Ablikim et al. (BES Collaboration), *Phys. Lett.* B607 (2005) 243.
12. B. S. Zou and D. V. Bugg, *Phys. Rev. D*48 (1993) 3948.
13. H. Q. Zheng et al., *Nucl. Phys.* A733 (2004) 235.
14. M. Ablikim et al. (BES Collaboration), *Phys. Lett.* B645 (2007) 19.
15. E. van Beveren et al., *Phys. Lett.* B641 (2006) 265; L.Roca et al., *Nucl. Phys.* A744 (2004) 127; G. Janssen et al., *Phys. Rev. D*52 (1995) 2690.
16. Q. Zhao, *Phys. Rev. D*72 (2005) 074001.
17. M. Ablikim et al. (BES Collaboration), *Phys. ReV. D*72 (2005) 092002.
18. M. Ablikim et al. (BES Collaboration), *Phys. ReV. D*70 (2004) 092002.
19. F. E. Close et al., *Phys.Rev. D*67 (2003) 074031; H. Nagahiro et al., arXiv:0803.4460 [hep-ph].